



HAL
open science

H2 storage with CO2 cushion gas in aquifers: Numerical simulations and performance influences in a realistic reservoir model

Sabrina Ben Rhouma, Alexandre Dos Santos, Fernanda de Mesquita L Veloso, Farid Smai, Pierre Chiquet, Roland Masson, Daniel Broseta

► To cite this version:

Sabrina Ben Rhouma, Alexandre Dos Santos, Fernanda de Mesquita L Veloso, Farid Smai, Pierre Chiquet, et al.. H2 storage with CO2 cushion gas in aquifers: Numerical simulations and performance influences in a realistic reservoir model. *International Journal of Hydrogen Energy*, 2025, 110, pp.101-114. 10.1016/j.ijhydene.2025.01.423 . hal-04954843

HAL Id: hal-04954843

<https://brgm.hal.science/hal-04954843v1>

Submitted on 18 Feb 2025

HAL is a multi-disciplinary open access archive for the deposit and dissemination of scientific research documents, whether they are published or not. The documents may come from teaching and research institutions in France or abroad, or from public or private research centers.

L'archive ouverte pluridisciplinaire **HAL**, est destinée au dépôt et à la diffusion de documents scientifiques de niveau recherche, publiés ou non, émanant des établissements d'enseignement et de recherche français ou étrangers, des laboratoires publics ou privés.



Distributed under a Creative Commons Attribution 4.0 International License



Contents lists available at ScienceDirect

International Journal of Hydrogen Energy

journal homepage: www.elsevier.com/locate/he

H₂ storage with CO₂ cushion gas in aquifers: Numerical simulations and performance influences in a realistic reservoir model

Sabrina Ben Rhouma ^{a,c,d} ,*,1, Alexandre Dos Santos ^b, Fernanda de Mesquita L Veloso ^a , Farid Smai ^a , Pierre Chiquet ^b, Roland Masson ^c, Daniel Broseta ^d

^a French Geological Survey (BRGM), 3 Av. Claude Guillemin - BP 36009, Orleans Cedex 2, 45060, France

^b TEREQA, 40 avenue de l'Europe, CS 20 522, 64010, Pau Cedex, France

^c University of Nice, 2004 route des Lucioles, BP 93 06902 Sophia Antipolis Cedex, France

^d Université de Pau et des Pays de l'Adour (UPPA), Pau, 64000, France

ARTICLE INFO

Keywords:

H₂ storage
CO₂ cushion gas
Operational scenarios
Injection rate
Heterogeneity

ABSTRACT

This paper presents the results of comprehensive numerical simulations utilizing the GEM modelling tool from Computer Modelling Group (CMG) to investigate the feasibility of seasonal Underground Hydrogen Storage (UHS) using CO₂ as the cushion gas in a realistic aquifer with a well-defined geological structure. The primary focus of the study is to address the challenge of efficiently recovering pure hydrogen (H₂) in UHS, as the contamination and recovery of the cushion gas significantly impact the economic viability of the project. The research aims to analyse and understand how various parameters, including operational, geological, and reservoir-related factors (e.g., injection and production rates, heterogeneity, gas solubility, etc.), influence the performance of the H₂ storage system, with the ultimate goal of identifying optimal storage scenarios.

The study evaluates the performance of a single injection and withdrawal well positioned at the summit of the anticline. The results highlight that the amount of recovered H₂ progressively increases with successive withdrawal cycles. Several parameters are found to influence the quality and quantity of the gas produced at this site, with geological heterogeneities playing a crucial role in attenuating up-coning effects. Notably, short-period cycles lead to an enhanced Hydrogen Productivity Index, while the production rate significantly impacts the quality of the produced gas and the mixing zone extent and location. The findings of this work demonstrate that H₂ storage can be achieved with reasonable gas recovery parameters. However, it is important to note that no geochemical considerations have been incorporated into this analysis.

1. Introduction

Renewable energies are not available all year-round due to weather conditions' fluctuation and the constraints imposed by their geographic location. Hydrogen (H₂) seems to be attracting global attention as a vector energy that can offer a low environmental impact solution and act as an energy carrier to overcome this seasonal shortage [1–3]. In order to reduce the energy curtailment, the excess production of renewable energy can be converted into H₂ by electrolysis and stored to be reused during periods of demand [4–8]. With the increased use of renewable sources to meet the Energy Transition Plan, large quantities of H₂ will be required, and surface storage facilities such as tanks and pipelines will come to their limits [9–11]. Therefore, Underground Hydrogen Storage (UHS) can offer many advantages, including capacity, safety, and economy [12–16]. Several storage geological structures

could be suitable, e.g., depleted gas reservoirs, salt caverns, and saline aquifers [17–23]. UHS in salt caverns has been the first to be tested and has proven its efficiency for short- to medium-term storage with the possibility of multiple injection and withdrawal cycles [24–27]. However, this type of storage has also proved to be limited in capacity and geographical distribution, as it requires the presence of evaporitic formations [28,29]. These limitations cannot be overlooked because the predicted demand for green energy in light of maximum energy decarbonizing is on the rise and alternatives are required [30]. UHS in porous media seems to be the most promising and inevitable solution to align with the transition strategy [31,32]. UHS in saline aquifers, which is the scope of this study, presents multiple challenges [33–35]. One of them is the production of water, and the insufficient pressure

* Corresponding author at: French Geological Survey (BRGM), 3 Av. Claude Guillemin - BP 36009, Orleans Cedex 2, 45060, France.

E-mail addresses: s.benrhouma@brgm.fr (S. Ben Rhouma), alexandre.dossantos@terega.fr (A. Dos Santos), f.veloso@brgm.fr (F. de Mesquita L Veloso), F.Smai@brgm.fr (F. Smai), pierre.chiquet@terega.fr (P. Chiquet), roland.masson@univ-cotedazur.fr (R. Masson), daniel.broseta@univ-pau.fr (D. Broseta).

¹ This is the first author footnote.

<https://doi.org/10.1016/j.ijhydene.2025.01.423>

Received 14 September 2023; Received in revised form 5 February 2024; Accepted 25 January 2025

0360-3199/© 2025 The Author(s). Published by Elsevier Ltd on behalf of Hydrogen Energy Publications LLC. This is an open access article under the CC BY license (<http://creativecommons.org/licenses/by/4.0/>).

required for production suggests the use of a Cushion Gas (CG). In this configuration, the aquifer consists of a CG that will be permanently stored, and the Working Gas (WG) is the gas that is injected and recovered during operational cycles, which in this case is H₂. Geological sites for carbon sequestration where the CO₂ is stored permanently would serve as an ideal CG candidate, offering potential cost savings. While CO₂ as CG has already been suggested in compressed air energy storage [36], its application in UHS remains relatively unexplored. In this specific context, the ratio CO₂ – H₂ is considered important information, yet its determination remains a challenge. Recently, the ratio CG/WG in UHS in aquifers was studied, particularly when the CG itself is H₂ [37]. The remaining challenge is to identify other geological but also operational parameters that could impact the mixing between the CG and the WG and have an effect on the cost-effectiveness of the project. In this study, a realistic geologic model of an actual natural gas reservoir is used as a case study. A sensitivity analysis of different parameters will be conducted to investigate their impact on the volume of gas produced and the degree of purity of this later. The temperature and pressure of the aquifer suggest that the system H₂ + CO₂ remains in the gas phase under storage conditions.

This paper begins with a summary of recently published numerical simulations work related to UHS in aquifers. It then presents the methodology used, including a detailed description of the reservoir, the base case scenario, and the relevant parameters considered in the simulations. The results of each parameter study are analysed and their impact on gas recovery and quality is discussed. The discussion section explores the impact of the combination of different factors and their effect on UHS performance. Finally, the conclusion summarises the main findings of the simulations, highlights effective scenarios, and suggests potential areas for further research.

2. Literature review

Previous research has extensively studied the UHS in aquifers using various simulation software. These studies have explored the capacity of storage systems, geochemical reactions, and the influence of various factors [38–42]. Some notable studies that have examined UHS in saline aquifers include the following:

- Comsol was used in a 3D model to study the well configuration for three annual cycles of UHS with H₂ as the CG for itself. The research estimated a maximum H₂ recovery rate of 78%, which is equivalent to a global energy efficiency of 30%. Notably, in this study, the CG was deemed unnecessary when H₂ was stored in steeply dipping structures. The major challenge identified in this storage was due to the coning effect and massive water intrusion. Efficient H₂ recovery was achieved when the production wells were shallow and located beneath the caprock [43].
- This work considered a hypothetical site with a realistic geological structure, using nitrogen (N₂) as the CG. They demonstrated the capacity of porous media to store significant quantities of H₂ and meet the required energy demands. The simulations were carried out using Eclipse (E300) [44].
- Using DuMux, this study explored the hydrodynamic effects of H₂ injection and compared them to methane CH₄. For hydrogen (H₂) storage, an initial amount of H₂ was injected into the reservoir. For the methane (CH₄) scenario, an equivalent amount of CH₄ was injected, although it was not explicitly designated as CG. It appears that at low injection rates, gravitational forces dominate, resulting in the uniform displacement of water by H₂. Conversely, at high injection rates, viscous forces became dominant, leading to unstable displacement. Notably, at higher injection rates, lateral fingering spreading of H₂ was observed to occur more rapidly than when CH₄ was injected [45].

- This work used TOUGH2 PetraSim to assess the feasibility of UHS (with H₂ as CG) in the Suliszewo aquifer in Poland. The authors concluded that the recovered amount of the total injected H₂ increases with the increase in the number of withdrawal cycles and highlighted the possible water management issue regarding the water withdrawn during H₂ production [46].
- This research investigated the impact of caprock availability and H₂ injection rate on H₂ recovery and leakage in UHS in a heterogeneous 3D model using TOUGH2. They revealed that the caprock presence and lower injection rates enhanced H₂ recovery, while higher injection rates increased H₂ leakage [47].
- This study focused on analysing the injection and storage of H₂ in an open saline aquifer, with a particular emphasis on investigating the role of H₂ CG. It was demonstrated that CG plays a significant role in controlling the injectivity of H₂ as well as influencing the storage capacity. In addition, geological parameters such as reservoir permeability and depth need to be taken into account when determining the capacity of CG as a WG in the aquifer [48].
- The study aimed to address unstable displacement and potential chemical reactivity caused by microorganisms consuming H₂. The model DuMuX was used to simulate the evolution of a hypothetical UHS system in a depleted gas reservoir and revealed that the hydrodynamic and biochemical effects are different compared to natural gas storage [49].
- In this paper, the authors leveraged data previously utilized to evaluate CO₂ storage potential in the UK, to assess H₂ storage capacity in gas fields and saline aquifers. They assumed a H₂ CG requirement of 50%. Through their sensitivity analysis, they determined that sites characterised by low temperatures and sealing rocks capable of withstanding high pressures are favoured locations for efficient storage [50].

Upon examination of the relevant studies, it became apparent that many of the literature studies do not consider the use of CG for UHS in aquifers. In most of these analyses, H₂ acts as a CG for itself, and there is no extensive numerical simulation study exploring UHS with CO₂ as a CG, particularly one carried out in a realistic geological model — this is a distinct advantage of the present work.

3. Methodology

The aim of this study is to conduct an extensive sensitivity analysis. The commercial simulation software GEM of Computer Modelling Group (a courtesy of CMG) [51] was used to model the non-isothermal and multi-phase flow (Eq. (1)) of a mixture of brine (water), CO₂, and H₂ in a realistic aquifer model. The used model served for natural gas storage and it is further discussed in the following first Section 3.1.

$$\phi \partial_t n_i + \text{div} \left(\sum_{\alpha \in \mathcal{P}} x_i^\alpha \zeta^\alpha \mathbf{q}^\alpha \right) = 0, \quad i \in C. \quad (1)$$

Here, ϕ is the porosity; n_i is the number of moles per unit pore volume (mol m⁻³), $n_i = \sum_{\alpha \in \mathcal{P}} S^\alpha C_i^\alpha \zeta^\alpha$; C_i^α is molar fractions; ζ is molar density (mol m⁻³); \mathbf{q} is generalized Darcy velocity (m s⁻¹); and \mathbf{q}^α is the velocity of each phase (m s⁻¹) given by the generalized Darcy's law.

A straightforward operational approach involves starting with a reservoir with CG that is already injected before proceeding with the injection and production of H₂. Therefore, the reservoir was initially filled with CG. Then, the reservoir was left shut-in for one month to reach equilibrium.

Afterward, some storage cycles with seasonal injection and withdrawal were simulated to represent a real case study where the operator plans to inject without a shut-in period after each operation. The injection and production data are depicted in the second Section 3.2.

The current model does not account for geochemical and bacterial reactions, and the methanation reaction is not activated. However, it

Table 1
Different reservoir rock types characteristics.

Rock type	Average porosity (%)	Average permeability (Darcy)	Lithology
1	30	4.6	Clean Sand
2	28	3	Clean Sand
3	24	0.092	Carbonated Sandstone
4	16	0.01	Degraded sandstone
5	7	0.00036	Poor reservoir facies

is crucial to consider these processes, as they involve methanogenic and acetogenic microorganisms capable of consuming H₂ and CO₂ to produce methane and acetate, respectively [52–54]. Geomechanics was not included to consider the changes in porosity and permeability, as well as the caprock integrity. The fluid behavior (PVT) is operated based on a cubic equation of state (PR1998) [55].

In this work, the analysis revolves around the base case as described in 3.2 and explores various scenarios by adjusting the input parameters mentioned in Section 3.3. The objective is to understand how these changes influence the purity and the H₂ volume recovered.

3.1. Reservoir description:

This study benefits from a realistic reservoir model based on the characteristics of a practical reservoir, capable of yielding results that closely resemble real-world situations in porous media. Petrel was utilized to generate the precise 3D static model.

The reservoir is an anticline, with the top located at a depth of 380 m below sea level, a temperature of 40 °C, and a hydrostatic pressure of 55 bar. The structure has an extent of 900 m and has an approximate thickness of 50 m. The water–gas contact is defined at 430 m. A hydrostatic pressure distribution is assumed throughout the reservoir, starting at this contact. The 3D structure of the reservoir is depicted in Fig. 1. The model consists of 213,180 grid blocks, with grid refinement around the well achieved by dividing each cell into 11x11x10 cells.

The model encompasses five different types of rocks, representing various horizons within the reservoir (Table 1). The lower part of the model simulates a substantial aquifer, enabling sufficient inflow or outflow volume to maintain the flow rates of the wells at the top. The aquifer is numerically simulated with a thickness of 200 m, a porosity of 0.25, and a permeability of 10 Darcy. The proportion of CG to WG initialized at the reservoir conditions has been determined to prevent water breakthrough during the back-production cycles. Therefore, the reservoir starts at 42 bar with 2.3E⁹ Stdm³ CG in place. In order to model the two-phase flow of CO₂-brine, relative permeability curves are employed from experimental data produced for CH₄-brine and tailored to different rock types as represented in Fig. 2s. While these curves are not specifically designed for CO₂, they provide a close approximation. The capillary pressure data was calculated using a standard Brooks & Corey function.

As a first approach, there is one well situated at the top layer of the structure, which serves as both an injection and production wells. The well perforations are located in the upper layer of the anticline. Injection and production flow rates are controlled based on pressure build-up and release, ensuring that the reservoir pressure remains within safe limits to prevent fracturing. The maximum and minimum allowable Bottom Hole Pressures (BHP) for injection and production are 100 bar and 1 bar, respectively. In the event of a violation of these BHP limits, the simulator automatically adjusts the well flow rate to bring the pressure within the specified range.

3.2. Base case scenario description:

A simplistic base case scenario was used as a reference (Fig. 1 left). This base case relies on a homogeneous layered model with equal vertical and horizontal permeability, ranging between 5 × 10⁻⁵ Darcy

Table 2
H₂ injection and production data.

Event	Event length (months)	Injection rate (Std m ³ /Day)	Production rate (Std m ³ /Day)
1	6	1,522,800	0
2	6	0	1,522,800

and 6 Darcy, and a porosity varying from 4% to 35% for different layers.

The reservoir is initially filled with brine, and the CG is introduced during the model setup. Following this, H₂ injection and production take place. The specific injection and production data are detailed in Table 2. There was no shut-in period between the injection and production phases. The simulation commences on 01-06-2023, and the well remains shut-in until the start of the H₂ injection phase on 01-07-2023. The project duration spans four years, ending on 28-06-2027.

3.3. Sensitivity analyses

When a CG other than the WG is used, diminishing mixing between the different gas components is a major challenge. The front spreading between the WG and the CG depends on the type of the CG chosen and the contrast of its physical properties compared to those of the WG. (the density, viscosity difference, and mobility ratio) and the coupled processes of molecular diffusion and mechanical dispersion. Molecular diffusion is a slow phenomenon that is generally proportional to the concentration gradient but also depends on the saturation, tortuosity, and the porosity of the reservoir. While the mechanical dispersion is governed by the velocity of the fluid.

The sensitivity analyses consist of changing the input parameters of the base case to investigate the impact of residual saturation, solubility of H₂ in the aqueous phase, diffusivity and diffusion, dispersion, reservoir heterogeneities, operational scenarios, and injection-well strategy.

3.3.1. Residual saturation

In underground storage processes, considering fluid-rock interactions is crucial, as they directly impact storage capacity and efficiency. When WG is stored in aquifers, the injection and withdrawal processes are controlled by WG-brine transport physics, involving “forced” drainage during injection and “spontaneous and forced” imbibition during withdrawal [56]. However, relative permeability hysteresis can have a dual effect: while it may reduce the H₂ withdrawal factor, it can improve the H₂ withdrawal purity [57]. Previous hysteresis trapping studies have shown that this parameter decreased the H₂ recovery factor by 0.37% in a single cycle of production and withdrawal when compared to their base case without hysteresis [58].

Here, the H₂ injection will be preceded by the injection of CO₂, which will come into contact with the brine. The CO₂-brine relative permeability curves significantly influence the capillary trapping of CO₂ in the reservoir, which has been extensively studied in various works related to carbon capture and storage [59]. With the presence of multiple gases, the hysteresis describing the relationship between gas saturation and pressure during injection and withdrawal is expected to become more complex.

In this study, CH₄-brine relative permeability curves were used, as H₂ – CO₂ brine relative permeability curves are not available.

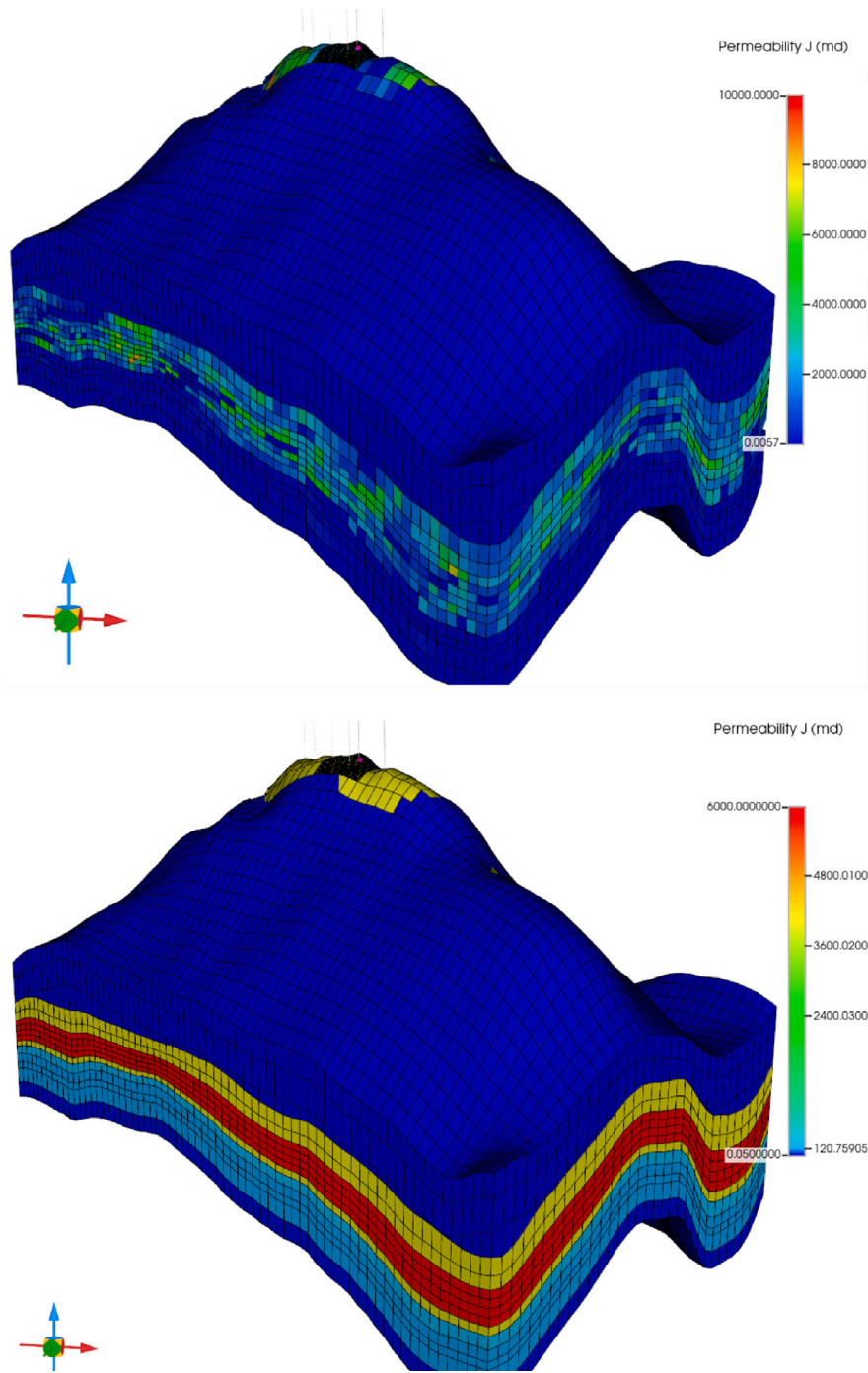


Fig. 1. Reservoir Model: horizontal permeability in both heterogeneous (left) and layered simple model: the base case (right).

3.3.2. Solubility in the aqueous phase

H₂ solubility was studied in saline solutions under reservoir conditions, and experimental data were used to supplement the lack of data for UHS. Various thermodynamic approaches have been developed to enhance the prediction of H₂ solubility and improve the models used in reservoir simulation software [60]. In the GEM simulation software, the gas solubility trapping in the aqueous phase was selected to be based on the general Henry’s law based on the fugacity formula, the equation is as the following:

$$f_{iw} = x_{iw} * H_i \tag{2}$$

where, x_{iw} is the mole fraction of the component $i = H_2$ in the aqueous phase, f_{iw} is the fugacity of the component (i) in the aqueous

phase and H_i is the Henry constant for the component, calculated as follows:

$$\ln H_i = \ln H_i^0 + \frac{v_i^\infty (P - P_i^0)}{RT} \tag{3}$$

H_i^0 is the reference Henry’s law constants of the components (kPa) at the reference pressure P_i^0 (kPa). v_i^∞ is the partial molar volume of the component i in the aqueous phase at infinite dilution (l/mol) and P is its partial pressure in the gas phase under equilibrium conditions, R is the gas constant, and T is temperature. The Henry constant is a function of pressure, where H₂ solubility in the aqueous phase increases with rising pressure and decreases with increasing temperature and salinity [61]. Comparatively, carbon dioxide exhibits the highest solubility in water

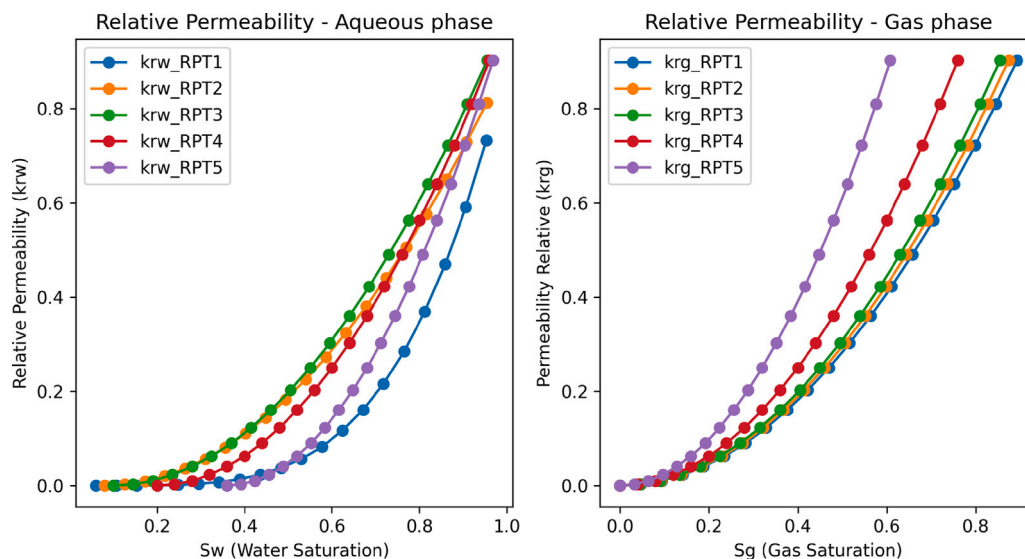


Fig. 2. Two-phases relative permeabilities for different rock types in the model. Left, the relative permeabilities as a function of water saturation. Right, the relative permeabilities as a function of the gas saturation. The different curves represent the five different rock types present in the model.

(0.169 g/100 g), followed by methane (0.0023 g/100 g), while H_2 has a very low solubility (0.00016 g/100 g) [62].

According to 63, the reference Henry's Law constant is set to 3.3×10^{-4} mol/m³Pa and 37.7×10^{-6} mol/m³Pa at a reference temperature of 298.15 K for CO_2 and H_2 , respectively.

Since CO_2 dissolution is a long process and could have a significant impact on the volume of the CG, in this work, it was preferred to also investigate the viability of the CG. Therefore, simulations were performed over a period of 10 years. The solubility of CO_2 was taken as a function of pressure, temperature, and salinity. The solubility model for CO_2 was enhanced by making the Henry's constant dependent on temperature, pressure, and salinity. The simulation results have already demonstrated the efficiency of this enhanced model for CO_2 , as they were compared to data from the literature [62].

The simulation for this parameter involved running the model with activated H_2 solubility and comparing it to the base case. Additionally, the impact of CO_2 solubility on the lifetime of the CG was assessed.

3.3.3. Dispersive phenomena

This section discusses the phenomena responsible for mixing.

(a) Physical Processes

Hydrodynamic dispersion, D , comprises molecular diffusion D_{mol} and mechanical dispersion D_{mech} , the main two processes controlling the mixing between the WG and the CG (Eq. (4)). Molecular diffusion dominates during quiescence, such as in scenarios with a shut-in period when there is no flow or exceedingly low flow. Conversely, mechanical dispersion predominates during periods of flow (injection or withdrawal). At reservoir scale, due to its dependency on velocity, hydrodynamic dispersion is a phenomenon that requires considering all flow mechanisms, including heterogeneity, as well as the influence of gravity on flow stability [64].

$$D = \tau D_{mol} + D_{mech}. \quad (4)$$

Where τ is the porous medium tortuosity.

Molecular diffusion. is usually considered a slow phenomenon that is proportional to concentration gradients [65]. The molecular diffusion process depends on the physical properties of the concerned molecule and the substrate (porosity, tortuosity, etc.). The molecular diffusion coefficient for H_2 in its gaseous state is relatively high, approximately 10^{-6} m²/s [66]. On the other hand, the diffusion coefficient for H_2 in

pure water is lower, estimated at 5.13×10^{-9} m²/s at 25 °C [23,67]. Comparatively, H_2 is more diffusive than CH_4 and CO_2 , with coefficients of 1.85×10^{-9} and 1.6×10^{-9} m²/s, respectively.

In previous studies on seasonal H_2 storage in depleted gas reservoirs, minimal H_2 losses due to dissolution and diffusion have been reported, reaching as low as 0.1% [23].

It is important to emphasize that in this case study, the reservoir is composed of a gas mixture, necessitating consideration not only of the diffusion of CO_2 in the aqueous phase but also that of H_2 in the gas phase.

In Section 4.3.1, we compare the base case with several scenarios where different molecular diffusion mechanisms are activated. One scenario involves the molecular diffusion of CO_2 , while the others focus on the diffusion of H_2 in the gas and water phases, and the final scenario encompasses both phenomena. By examining these scenarios, we aimed to understand the impact of molecular diffusion on the storage process and the overall behavior of the reservoir.

Mechanical dispersion. The mechanical dispersion phenomenon is initiated by the movement of fluid in porous media, which is primarily influenced by the flow velocity and direction [66]. Accurately predicting the mechanical dispersion process necessitates characterizing the dispersivity coefficient of the field site. However, this parameter is challenging to determine due to the laboratory's incapacity to reproduce such irregularities (mainly natural heterogeneities that cause irregular flow at the field scale). Laboratory measurements typically identify dispersivity coefficients at the scale of a few millimeters or centimeters. Nevertheless, field tracer tests can be employed to determine the mechanical dispersion coefficient [65].

The simulations were conducted (Section 4.3.2) with varying dispersivity coefficient values ranging from a few centimeters to meters. The choice of an intentionally high and probably non-realistic dispersivity coefficient for this site was made to investigate the effect of increased dispersion. It is worth noting that in this study, the longitudinal and transverse dispersivity coefficients remain the same for all layers.

(b) Numerical impact

If the hydrodynamic process is disabled in the model, numerical dispersion is likely to still be effective in the simulation, causing the observed mixing effect between the two gases. Although inherent to the approximation of modelling techniques, numerical dispersion can be compared to hydrodynamic dispersion. Typically, hydrodynamic dispersion values in porous aquifers are within the range of 10–100

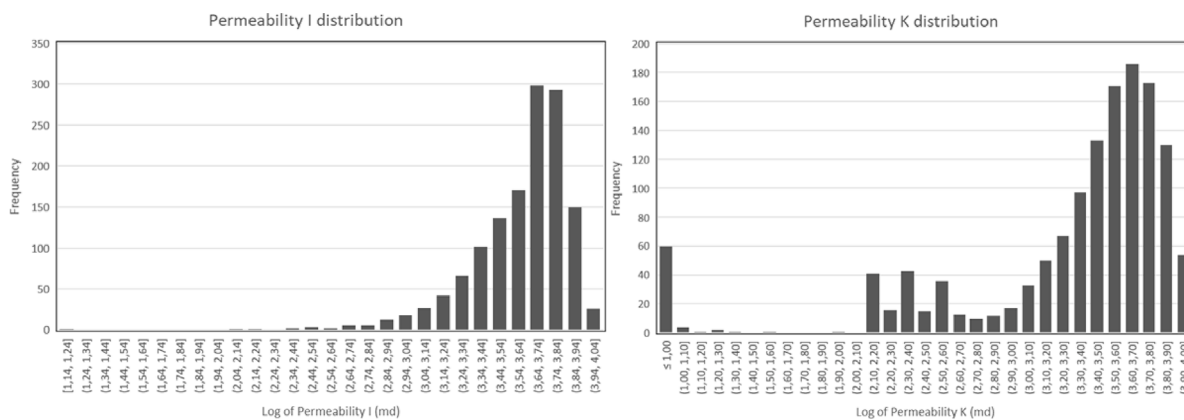


Fig. 3. Permeability distribution for both Horizontal (left) and vertical direction (right).

Table 3
H₂ Operational schedule data.

scenario	Event length (months)	Injection rate (Std m ³ /Day)	Shut-In (months)	Event length (months)	Production rate (Std m ³ /Day)
A (Base case)	6	1,522,800	0	6	1,522,800
B	3	1,522,800	0	3	1,522,800
C	3	1,522,800	3	3	1,522,800
D	6	1,522,800	0	6	761,400
E	6	1,522,800	0	6	507,600
F	6	761,400	0	6	1,522,800
G	6	761,400	0	6	761,400

meters [36,68]. In some cases, the numerical dispersion can be substantial enough to completely dominate the true physical dispersion. Reducing the size of the cells, especially in the front contact zone, can help mitigate the numerical dispersion.

Comparing simulations in which mechanical dispersion is enabled with simulations where this process is disabled will enable an evaluation of numerical dispersion.

In this section, the reference case that will be used is the base case, including heterogeneity defined in the next section.

3.3.4. Geological heterogeneities

In previous works, it was highlighted that the impact of the CG on the recovery process was closely related to the permeability of the reservoir [58]. In fact, geological heterogeneities are a factor that can significantly impact the dispersion of the fluid in porous media. A geostatistically distributed heterogeneous model of the permeability field was used. The model consists of five different rock fluid types with different levels of heterogeneity Fig. 3. The porosity was also distributed across the different layers, and it ranges from 0.07 to 0.3.

3.3.5. Operational scenario

The base study involved multiple storage injection and withdrawal cycles with constant rates. In this section, we will explore the reservoir's performance by evaluating operational parameters and studying their impact on the storage process. The injection rate, production rate, and time interval of the process will be modified, as shown in Table 3. Each scenario is defined by its event length, injection rate, shut-in duration, and production rate. Scenario A (base case) maintains a seasonal event length without shut-in periods, injecting and producing H₂ at a constant rate. Scenario B and scenario C both have an event length of 3 months and the same injection and production rates as scenario A. The difference arises in scenario C, where a shut-in duration of 3 months is introduced. In contrast, scenario D maintains a 6-month event length with the same injection rate as the base case, but halves the production rate. Similarly, scenario E maintains the 6-month event length and injection rate but reduces the production rate by a third of the production case of the base case. Scenario F deviates in its injection

rate, operating at half the rate of the base case, while maintaining a 6-month event length and no shut-in period. Lastly, scenario G mirrors scenario F, equalizing both the injection and production rates at half of the rates seen in the base case.

3.3.6. Well configuration

For the sake of simplicity, the base case in this study involves a single well that serves both as an injector and producer through the same perforations. Inspired by the selective technology [45], which involves deep perforation injection and shallower perforation production, we also explore a dual-well configuration. In this arrangement, one well operates as an injector at a greater depth, while the other serves as the producer at a shallower level. This study evaluates the effectiveness of these distinct scenarios.

Scenario A represents the base case with a single well configuration, while Scenario H explores a model with two distinct wells for injection and production, as explained earlier. Scenario I replicates the base case but with a reduced production rate, and Scenario J follows the dual-well concept with a reduced production rate as well.

The impact of perforation location on the recovery of H₂ is also investigated in this section, considering the findings that shallower perforations may influence the injection process [37]. This section will explore the impact of the perforations' location on the recovery of H₂.

4. Results

For all the treated scenarios, the hydrodynamics of the H₂ plume reflect the density contrast between H₂ and CO₂, as demonstrated by the upward migration of H₂ beneath the caprock. The anticline structure of this model enhances the accumulation of H₂ and prevents its lateral spreading. In this section, we will discuss the impact of the previously mentioned parameters on the efficiency of H₂ storage and recovery.

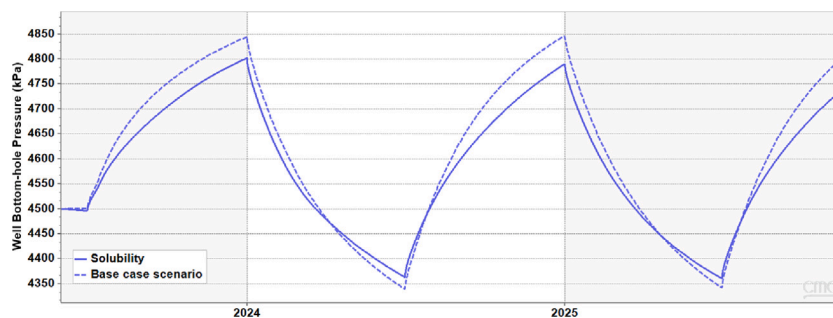


Fig. 4. Comparison of bottom-hole pressure between the base case model and the model with solubility of H_2 and CO_2 activated.

4.1. Effect of hysteresis

The hysteresis trapping was added to the base case to investigate its potential impact on production behavior. The hysteresis did not affect the recovery factor of H_2 when compared to the base case. Similarly, when heterogeneity was applied to the base case and to the base case with hysteresis, it also did not seem to have a notable impact on the results. The unchanged behavior observed in both cases was actually expected, as the input data does not consider the mixture of gases and is primarily controlled by gas displacement around the well (driven by the mobility ratio), which is far from the water contact (even though it may indirectly influence the reservoir).

4.2. Effect of solubility in the reservoir

Solubility is considered an important process since even a small amount of H_2 dissolved in water can trigger biological activity [45]. Numerical simulations were conducted with H_2 solubility activated and compared to the base case scenario. However, negligible impacts were observed on the volume and purity of the H_2 produced. On the other hand, the solubility had a slight impact on the bottom-hole pressure of the injection-production well, as depicted in Fig. 4. Activating the solubility model resulted in a small reduction in the bottom-hole pressure due to the dissolution of gases in the aqueous phase within the reservoir.

Evaluating the effect of CO_2 dissolution on H_2 recovery is complex. The solubility of CO_2 is important, and it may lead to a relatively slow consumption of the CG, subsequently affecting the pressure provided by this gas to ensure the necessary pressure required for production. After 5 years, the well pressure dropped by 0.8% of its initial pressure. Further investigation may be needed to determine whether a refill of the CG is required, depending on the potential time scales of the storage.

Due to the negligible effect of H_2 solubility and the computational time required by the CO_2 solubility model, we have not considered this process in the subsequent simulations conducted in this study.

4.3. Effect of dispersive phenomena

4.3.1. Effect of molecular diffusion

The modelling process, taking into account diffusion, was time-consuming, with convergence difficulties due to the complexity of the problem. Despite this challenge, simulations were conducted considering the molecular diffusion of H_2 in gas using the Sigmund correlation [69], and the molecular diffusion coefficient of H_2 and CO_2 in the aqueous phase was also taken into account, along with the presence of reservoir heterogeneity.

Accounting for diffusion in the gas and the aqueous phase did not significantly impact the results compared to the same case when diffusion was deactivated. This finding suggests that other dominant factors may overshadow the influence of molecular diffusion in the gas and aqueous phases. However, it is important to acknowledge that this parameter should not be overlooked in further investigations, even though it is common to deactivate it in simulations.

4.3.2. Effect of mechanical dispersion

Fig. 5 represents the H_2 mole fraction and the cumulative gas volume during the first production cycle. Various curves are present, each representing a different dispersivity coefficient, alongside the curve for the reference case. It is evident that the degree of mixing is notably influenced by the dispersivity coefficient. The H_2 mole fraction in the produced gas consistently remains below or equal to the H_2 mole fraction produced in the base case, although these values approach the base case values as the cycle nears its end. The same behavior is observed for cumulative gas withdrawal. This indicates that an increasing value of the dispersivity coefficient leads to pronounced mechanical dispersion, consequently increasing the mixing of CO_2 with H_2 . The simulation conducted with a dispersivity coefficient of 0.10 meters nearly overlaps the reference case curve, suggesting that numerical dispersion is very small. This is mainly due to local grid refinement around the well and in the contact zone between the two fluids.

When the dispersivity coefficient was set to greater than 1 meter, the impact of mechanical dispersion became significant. The 2D reservoir view in Fig. 6 illustrates the H_2 mole fraction at the midpoint of the production period. Comparing the two profiles, it is evident that the H_2 fraction in the model with activated mechanical dispersion (Fig. 6, left) is notably lower than in the base model with heterogeneity (Fig. 6, right). Only a small portion of pure H_2 remains trapped beneath the cap rock.

The dispersion coefficient for the relevant site of our study appears to be on the order of 1 meter, and the mechanical effect of this value is not significant. Therefore, within the context of this research, numerical dispersion will be considered analogous to mechanical dispersion.

Mechanical dispersion is closely linked to flow velocity. Reduced velocities at greater distances from the well diminish the dispersion effect [36]. This aligns with other research highlighting the significant impact of injection and production rates on mixing between nitrogen and methane [70]. Therefore, the mixing observed here may be minimized by reducing injection and production rates. It is important to note that, alongside molecular diffusion, mechanical dispersion amplifies the mixing of gas components [66].

However, it is important to mention that activating this parameter significantly increases computational time for the simulator (requiring up to 48 h to simulate 300 days, compared to an average of 15 h) and often leads to convergence challenges. Despite its importance, the substantial time cost associated with activating this parameter makes it unfeasible to conduct simulations for testing purposes.

4.4. Effect of heterogeneity

As can be observed in Fig. 7, during production in the base case scenario, the amount of H_2 stored in the aquifer decreases unless the wells are shut down due to upconing (see Fig. 8 right).

The CG/WG mixing zone reaches the production well, leading to an increase in CO_2 mole fraction production in the lower part of the well. This negatively impacts the efficiency of H_2 production, as the injected H_2 tends to rise and becomes less abundant in the lower regions.

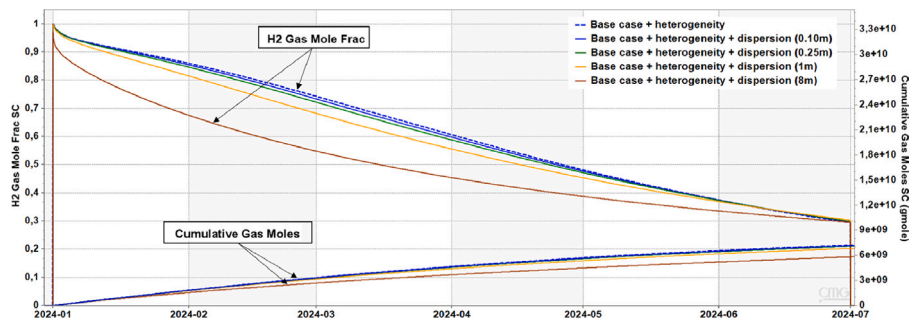


Fig. 5. H₂ mole fraction recovered and cumulative H₂ mass produced-impact of activating mechanical dispersion.

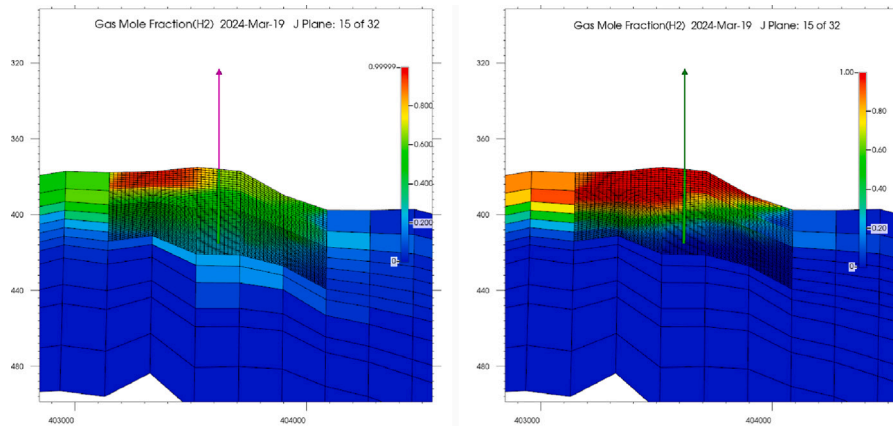


Fig. 6. IK 2D view representing the H₂ mole fraction comparison between the mechanical dispersion (8 m) activated model (left) and the heterogeneous base case (right). The focus is on evaluating the impact of diffusion.

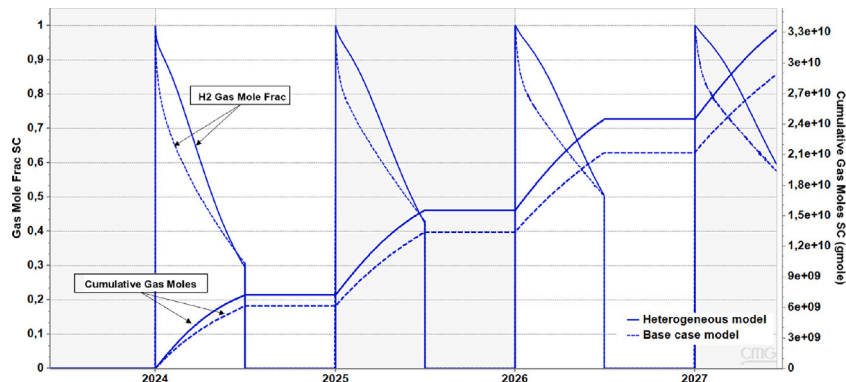


Fig. 7. H₂ mole fraction recovered and cumulative H₂ mass produced-impact of adding heterogeneity.

When the heterogeneity of this model is introduced, the heterogeneous permeability field significantly impacts well productivity, especially due to the effect of vertical permeability on coning. As depicted in Fig. 7, before reaching the same H₂ mole fraction at the end of each cycle, we achieve a higher H₂ mole fraction with the heterogeneous model. This is further confirmed by the cumulative withdrawn volume of H₂, which is higher for the heterogeneous case. The mitigation of the coning effect due to the incorporation of this reservoir heterogeneity is illustrated on the left side of Fig. 8. Heterogeneity, in this case, promotes a non-uniform gas distribution [44].

4.5. Effect of the operation strategy

The injection and production rate, as well as the cycle duration (Fig. 9) have a significant impact on both the quality and quantity of the produced H₂.

Among the scenarios, E and G represent the highest and lowest mole fractions of H₂ recovery at the end of the production cycle, respectively. When compared to the base case, scenarios C, F, and G exhibit a lower H₂ fraction in the produced gas, as well as less cumulative volume. Conversely, scenarios E and D exhibit a better H₂ mole fraction compared to the base case, albeit with different cumulative volumes (D has more volume than E). Notably, scenario B represents the only case with both an improved H₂ fraction and cumulative volume.

In scenarios F and G, the quantity of injected H₂ is reduced, however, reducing the production rate, as in case G, seems to enhance the quality of the produced gas. For instance, producing at half the rate of the injection rate leads to 62.4% of the base case quantity produced, while producing at a rate equivalent to one-third of the injection rate results in 45.2% of the base case quantity produced for the same injection-production cycle period.

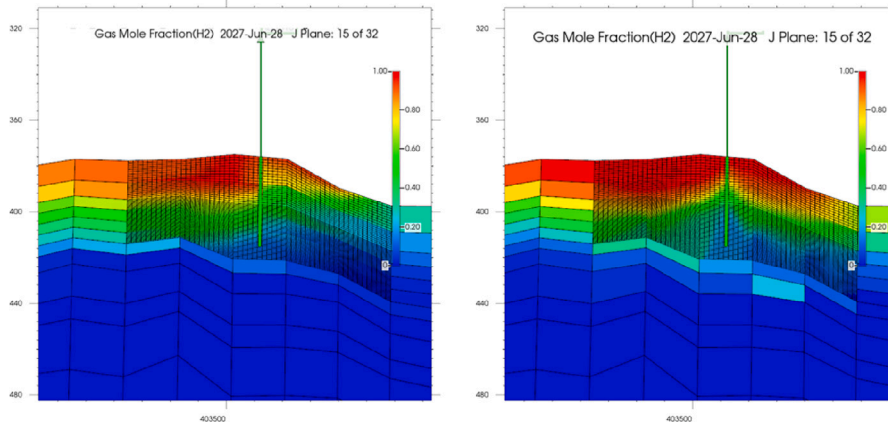


Fig. 8. IK 2D view representing the H₂ mole fraction comparison between the heterogeneous model (left) and the base case (right). The focus is on evaluating the impact of reservoir heterogeneities.

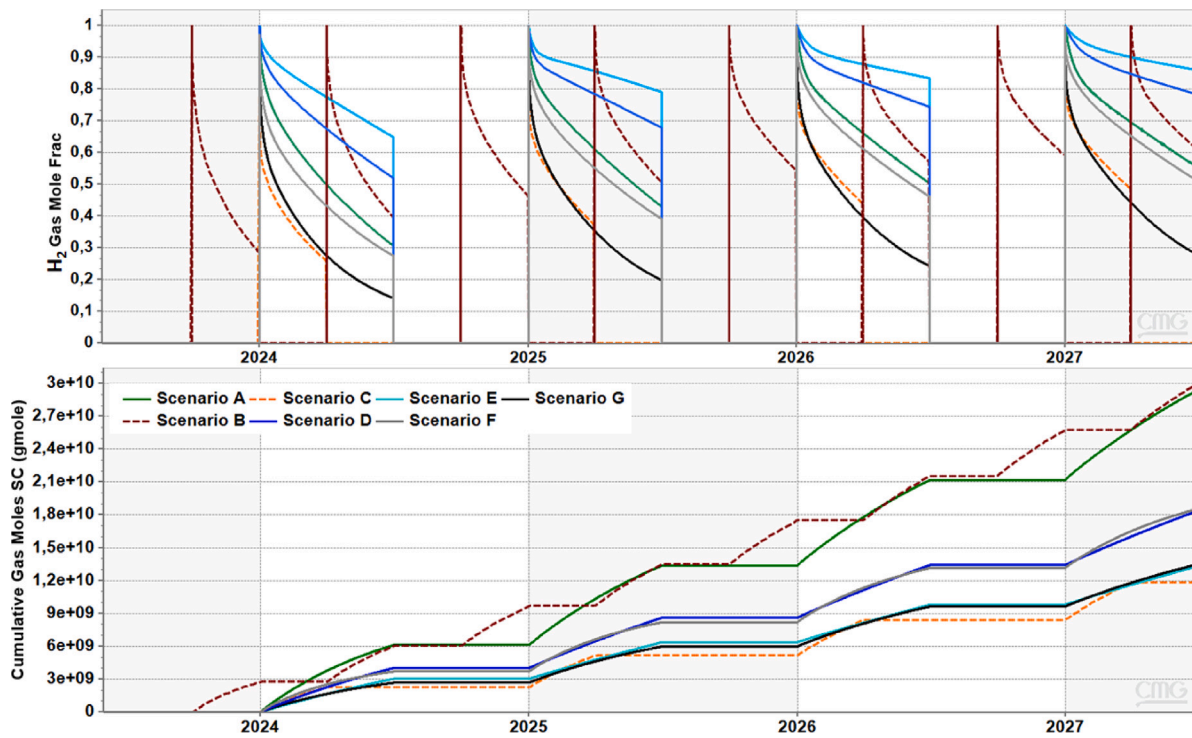


Fig. 9. H₂ gas fraction withdrawn for every considered scenario (up) and the corresponding cumulative H₂ gmole (down)- Effect of the operation strategy.

Scenarios B and G represent the same quantities injected and withdrawn, but over different periods of time and at different rates. In Scenario B, double the quantity is injected and withdrawn compared to Scenario G, but within half the time frame. Comparing these two scenarios highlights the impact of the injection rate on the reservoir dynamics, illustrating a trade-off between gravity segregation and viscous fingering.

Gravity override is predominantly observed in most cases, with H₂ naturally tending to migrate to the top of the structure. This displacement is dependent on the velocity and can become unstable at a critical velocity, thereby affecting gas distribution, as depicted in Fig. 10 [71].

In Fig. 11, the left side illustrates the H₂ fraction in Scenario B after 3 months of injection, while the right side shows the same for Scenario G after 6 months of injection. This figure represents the gas distribution beneath the caprock. Notably, when the injection rate is lower, the lateral spread is more significant due to the prevailing gravitational

forces.

Scenario C presents a case with both low quality and quantity, mainly due to the shut-in period. Interestingly, the rest time between operations not only enhances mixing but also provides time for H₂ to migrate laterally beneath the caprock. This migration reduces the vertical height of the H₂ layer under the caprock and increases the contact of the CO₂ fraction with the well perforation, as illustrated in Fig. 12. The left view is depicted immediately after the injection phase of scenario B, while the right view shows the situation one month after the injection phase.

During the shut-in period, as observed in the figure, gravity forces had sufficient time to establish layering based on density, leading to a change in the shape of the plume around the well.

The most favorable scenario appears to be when reducing the injection and withdrawal periods. However, it remains uncertain whether this approach is practical for real-case applications and whether it

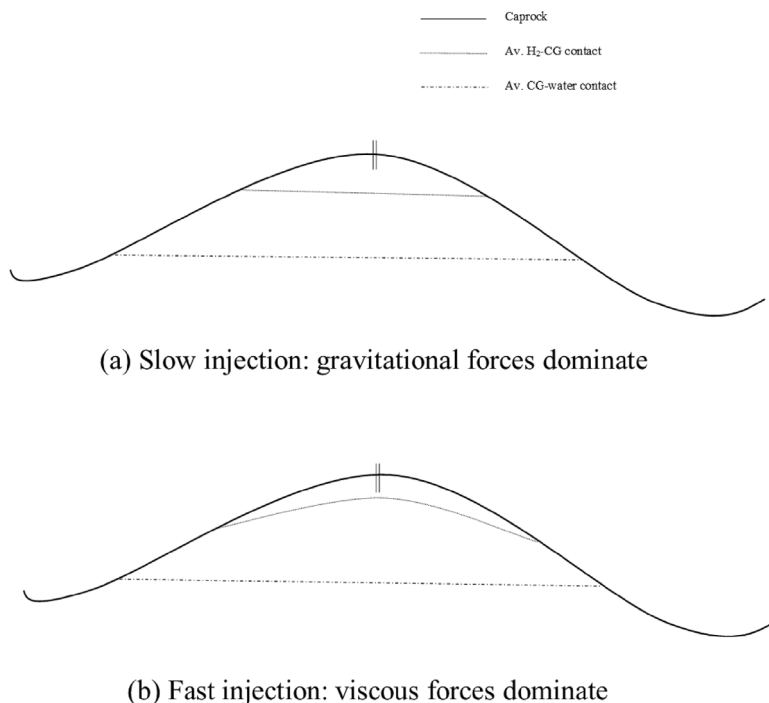


Fig. 10. A schematic representation of the gas spreading depending on the injection rates. Source: Figure modified from [71].

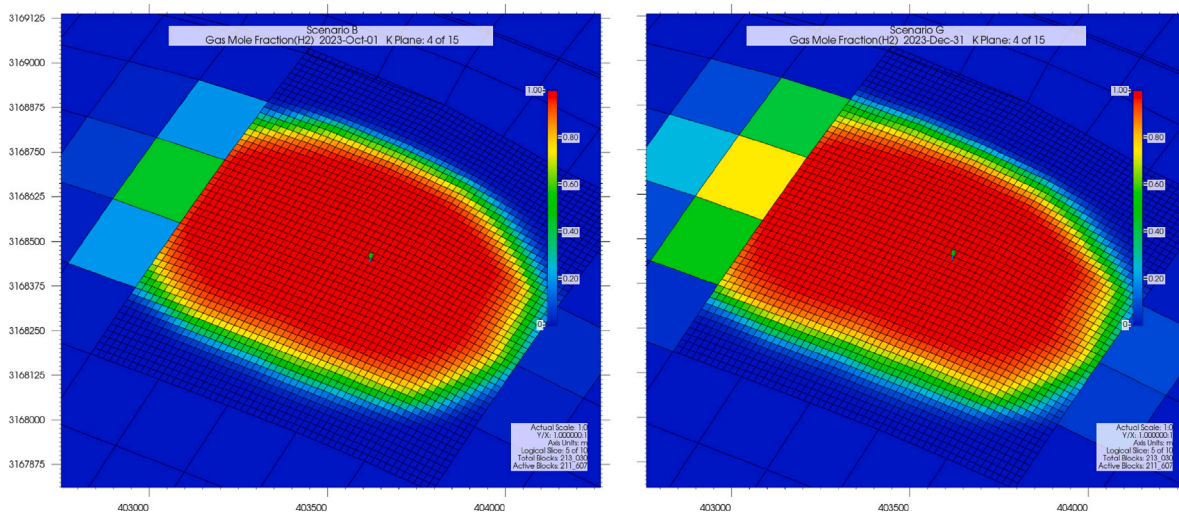


Fig. 11. Plane view depicting a comparison of H₂ mole fraction between scenario B (left) and scenario G (right). The visual highlights the distinct variations in H₂ distribution resulting from the difference in injection rate.

aligns with seasonal storage plans.

4.6. Effect of well configuration

The results, as shown in Fig. 13, indicate that the use of different perforations in Scenarios H and J did not have a substantial impact on either the fraction or the quantity of produced H₂ when compared to the base cases (Scenarios A and I, respectively).

Scenario H closely resembles Scenario A, with the H₂ fraction and cumulative volume of produced gas exhibiting minimal differences. Similarly, Scenario J closely mirrors Scenario I, with slight variations in the H₂ fraction and cumulative volume.

These findings suggest that the concept of employing deep perforations for injection and restricting production to the upper part of the

reservoir did not significantly alter the overall performance of the H₂ storage process. However, these slight differences observed between scenarios may still carry practical implications that require further investigation for real applications.

5. Discussion

Based on the above sensitivity study, we identified the most significant parameters with a considerable impact on gas purity and/or quantity. These key parameters include heterogeneity, production rate, and cycle duration. In this section, we conducted simulations by combining two or three of these identified processes, as outlined in Table 4.

The main goal of these simulations is to determine the most effective scenario by evaluating the combined effects of these parameters.

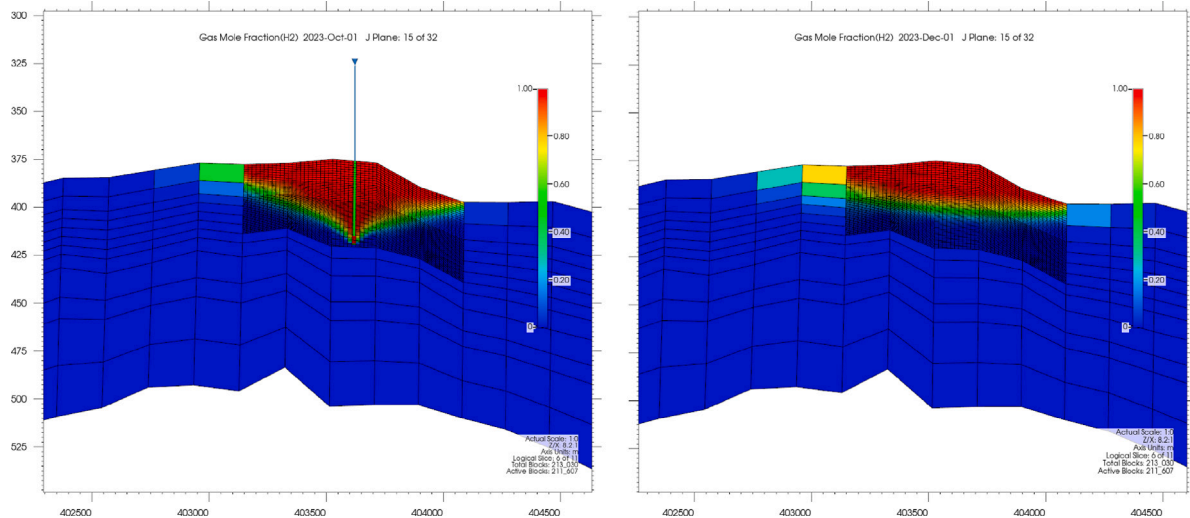


Fig. 12. IK 2D view depicting a comparison of H₂ mole fraction between scenario B (left) and scenario C (right). The visual highlights the distinct variations in H₂ distribution resulting from the different operational conditions, showcasing the effects of the shut-in period in scenario C.

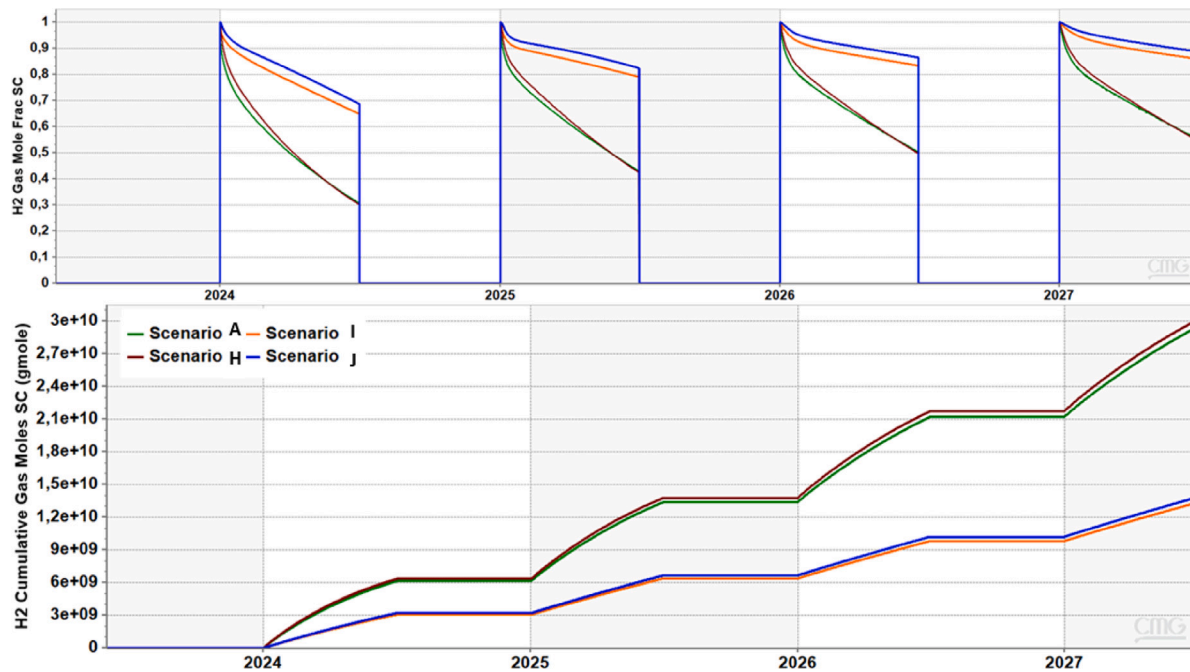


Fig. 13. H₂ gas fraction withdrawn for every considered scenario (up) and the corresponding cumulative H₂ gmole (down)- Effect of the well configurations.

To assess the effectiveness of each scenario, we employed a Hydrogen Productivity Index, defined as the ratio of cumulative H₂ produced to cumulative H₂ injected (Eq. (5)).

$$H_2 \text{ productivity index} = \frac{\text{Cumulative } H_2 \text{ produced}}{\text{Cumulative } H_2 \text{ injected}} \times 100 \quad (5)$$

Additionally, the withdrawal quality of H₂, expressed as a gas mole fraction of the total gas produced, complements this recovery factor. These parameters collectively serve as crucial metrics for evaluating the performance of each scenario in terms of H₂ recovery during the storage process.

Fig. 14 showcases two plots. On the left, we observe the H₂ mole fraction selected at the end of the withdrawal period and its corresponding standard cumulative gas produced volume. The cycle numbers are also indicated on the curves. This plot reveals two distinct reservoir behaviors: one that delivers large volumes (composed of less

than 70% H₂) and other behavior that delivers higher-quality gas but with a limited volume due to a reduced production rate. Scenarios A, B', C', and E' are associated with delivering large volumes, whereas scenarios D', F', and G' focus on delivering high-quality gas.

On the right side, we present a graph illustrating the H₂ Productivity Index's behavior over time. Notably, scenarios B', C', and E' exhibit higher productivity indices, indicating that despite not having the best gas quality, a significant quantity of the injected H₂ is effectively recovered. It is important to highlight that the quality of the produced H₂ improves with each cycle, a trend consistent with findings from other studies. Towards the end of the last cycle, scenarios B' and E' surpass a productivity index of 70%, making them potential economically viable and practical options for real-world applications.

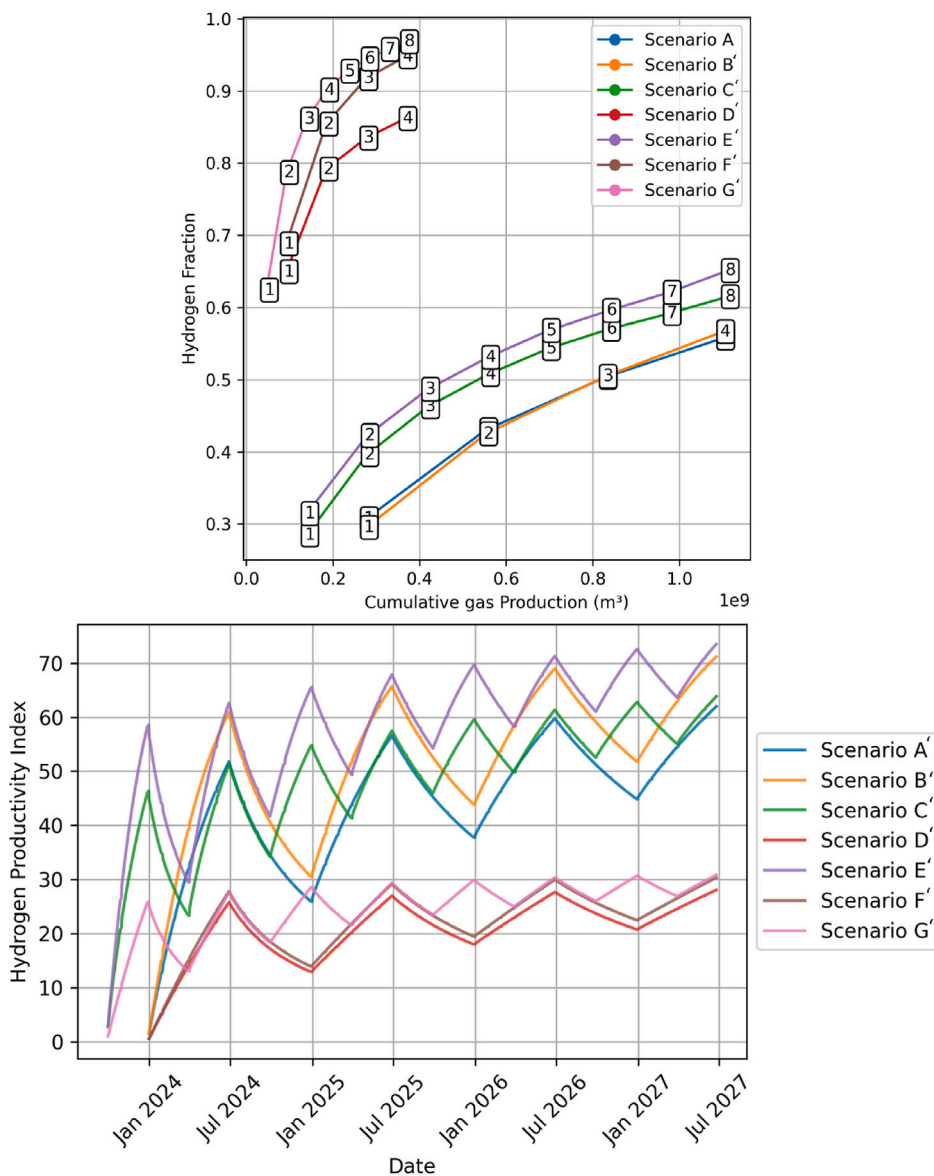


Fig. 14. Dynamics of H₂ Productivity. Left: H₂ mole fraction at the end of the withdrawal period and the corresponding standard cumulative volume of the produced gas. The numbers represent the cycle numbers. Right: the H₂ productivity index as function of time.

6. Conclusions and prospects

This study has focused on investigating the key parameters that impact the viability and effectiveness of UHS in aquifers, using CO₂ as a CG, through numerical simulations. Various scenarios were explored by adjusting input parameters, such as residual saturation, H₂ solubility in the aqueous phase, diffusion, dispersion, reservoir heterogeneities, operational scenarios, and injection-well strategy, to understand their influence on gas recovery and quality. The simulations revealed that heterogeneity, cycle duration, and production rate play crucial roles in enhancing gas quality and cumulative recovered volume.

- Heterogeneities enhanced the quality of the recovered gas by suppressing the coning effect. Note that this finding is site-specific.
- Producing at a slower rate, while keeping the injection rate and period constant, effectively reduces the mixing between the two gases. This results in the mixing zone being pushed further

away from the well, allowing for the production of less contaminated H₂. This conclusion is consistent with findings from other studies [72].

- Reducing the cycle duration helps to quickly recover the injected H₂ and limits the time for the gas to migrate and mix.
- Mechanical dispersion can have a significant impact on the mixing zone, and its effect closely depends on the dispersivity coefficient. Characterizing this parameter for each specific site is essential for assessing the profitability of the storage project.

To evaluate the combined effects of these parameters, the H₂ Productivity Index was analyzed. The scenario with heterogeneity and an increased number of cycles per year demonstrated higher efficiency. Furthermore, it was observed that gas quality improves with each cycle, potentially reaching economically viable levels by the end of the last cycle in certain scenarios. However, further investigations are recommended to explore the long-term behavior of gas quality and stability over extended simulation periods.

Table 4
Simulations details.

Process	Heterogeneity	Event length ^a	Production rate ^b
Scenario B'	X		
Scenario C'		X	
Scenario D'			X
Scenario E'	X	X	
Scenario F'	X		X
Scenario G'	X	X	X
Scenario B'	X		
Scenario C'		X	
Scenario D'			X
Scenario E'	X	X	
Scenario F'	X		X
Scenario G'	X	X	X

Scenario A is the base case defined earlier in this work.

^a The event length is reduced from 6 months to 3 months of injection and 3 months withdrawal.

^b The production rate is defined as third of the injection rate 507600 Std m³/Day.

The challenge at UHS lies in striking a balance between the quality and quantity of the produced gas. Achieving high gas quality often requires accepting a lower gas quantity, and vice versa. Therefore, it is essential to conduct an economic analysis, which involves calculating the levelized cost of hydrogen storage, taking into account both the CapEx (Capital Expenditure) and OpEx (operational expenditure) factors [73]. CapEx includes the initial investment costs, such as the cushion gas investment, while OpEx covers ongoing operational costs from the first day of the project.

By integrating technical insights from this study with the economic analysis, better decision-making and planning can be achieved in industrial applications. This approach can help identify promising scenarios for efficient and cost-effective UHS solutions.

Declaration of competing interest

The authors declare that they have no known competing financial interests or personal relationships that could have appeared to influence the work reported in this paper.

Acknowledgments

This research was co-funded by BRGM and Terega. The authors extend their sincere gratitude to these organizations for their generous support in funding the PhD program and providing invaluable resources throughout the research. Additionally, the authors are thankful to CMG for granting a license to use the GEM simulation tool, which was crucial to the success of this work.

References

- [1] Sgobbi A, Nijis W, De Miglio R, Chiodi A, Gargiulo M, Thiel C. How far away is hydrogen? Its role in the medium and long-term decarbonisation of the European energy system. *Int J Hydrog Energy* 2016;41(1):19–35.
- [2] Ma J, Li Q, Kühn M, Nakaten N. Power-to-gas based subsurface energy storage: A review. *Renew Sustain Energy Rev* 2018;97:478–96.
- [3] Fonseca JD, Camargo M, Commenge J-M, Falk L, Gil ID. Trends in design of distributed energy systems using hydrogen as energy vector: A systematic literature review. *Int J Hydrog Energy* 2019;44(19):9486–504.
- [4] Crotogino F, Donadei S, Bünger U, Landinger H. Large-scale hydrogen underground storage for securing future energy supplies. In: 18th world hydrogen energy conference, vol. 78. 2010, p. 37–45.
- [5] Owen A, Garniati L. Chapter 25 - The politics of investing in sustainable energy systems. In: Letcher TM, editor. *Storing energy*. Oxford: Elsevier; 2016, p. 529–38.
- [6] Maggio G, Nicta A, Squadrito G. How the hydrogen production from RES could change energy and fuel markets: A review of recent literature. *Int J Hydrog Energy* 2019;44(23):11371–84.

- [7] Hanley ES, Deane J, Gallachoir BO. The role of hydrogen in low carbon energy futures—A review of existing perspectives. *Renew Sustain Energy Rev* 2018;82:3027–45.
- [8] El-Shafie M, Kambara S, Hayakawa Y. Hydrogen production technologies overview. *J Power Energy Eng* 2019;7(1):107–54, Number: 1 Publisher: Scientific Research Publishing.
- [9] Delmastro C, Lavagno E, Schranz L. Energy and underground. *Tunn Undergr Space Technol* 2016;55:96–102.
- [10] Abdalla AM, Hossain S, Nisfindy OB, Azad AT, Dawood M, Azad AK. Hydrogen production, storage, transportation and key challenges with applications: A review. *Energy Convers Manage* 2018;165:602–27.
- [11] Astiaso Garcia D, Barbanera F, Cumo F, Di Matteo U, Nastasi B. Expert opinion analysis on renewable hydrogen storage systems potential in Europe. *Energies* 2016;9(11):963, Number: 11 Publisher: Multidisciplinary Digital Publishing Institute.
- [12] Carden P, Paterson L. Physical, chemical and energy aspects of underground hydrogen storage. *Int J Hydrog Energy* 1979;4(6):559–69.
- [13] Matos CR, Carneiro JF, Silva PP. Overview of large-scale underground energy storage technologies for integration of renewable energies and criteria for reservoir identification. *J Energy Storage* 2019;21:241–58.
- [14] Olabi AG, bahri As, Abdelghafar AA, Baroutaji A, Sayed ET, Alami AH, et al. Large-vs-scale hydrogen production and storage technologies: Current status and future directions. *Int J Hydrog Energy* 2021;46(45):23498–528.
- [15] Verga F. What's conventional and what's special in a reservoir study for underground gas storage. *Energies* 2018;11(5):1245, Number: 5 Publisher: Multidisciplinary Digital Publishing Institute.
- [16] Audigane P, Bader A, Gentier S, Beccaleto L, Bellenfant G. The role of the underground for massive storage of energy: a preliminary glance of the French case. 2014, The EGU General Assembly.
- [17] Micioc J, Heinemann N, Edlmann K, Scafidi J, Molaei F, Alcalde J. Underground hydrogen storage: a review. *Geol Soc Lond Spec Publ* 2023;528(1):SP528–2022–88, .
- [18] Tarkowski R. Underground hydrogen storage: Characteristics and prospects. *Renew Sustain Energy Rev* 2019;105:86–94.
- [19] Hematpur H, Abdollahi R, Rostami S, Haghighi M, Blunt MJ. Review of underground hydrogen storage: Concepts and challenges. *Adv Geo- Energy Res* 2023;7(2):111–31, .
- [20] Song H, Guo H, Wang Y, Lao J, Zhu H, Tang L, et al. A novel hybrid energy system for hydrogen production and storage in a depleted oil reservoir. *Int J Hydrog Energy* 2021;46(34):18020–31.
- [21] Muhammed NS, Haq B, Al Shehri D, Al-Ahmed A, Rahman MM, Zaman E. A review on underground hydrogen storage: Insight into geological sites, influencing factors and future outlook. *Energy Rep* 2022;8:461–99.
- [22] Bünger U, Michalski J, Crotogino F, Kruck O. 7 - Large-scale underground storage of hydrogen for the grid integration of renewable energy and other applications. In: Ball M, Basile A, Veziroglu TN, editors. *Compendium of hydrogen energy*. Woodhead publishing series in energy, Oxford: Woodhead Publishing; 2016, p. 133–63. <http://dx.doi.org/10.1016/B978-1-78242-364-5.00007-5>, URL <https://www.sciencedirect.com/science/article/pii/B9781782423645000075>.
- [23] Amid A, Mignard D, Wilkinson M. Seasonal storage of hydrogen in a depleted natural gas reservoir. *Int J Hydrog Energy* 2016;41(12):5549–58.
- [24] Pfeiffer WT, Bauer S. Subsurface porous media hydrogen storage – Scenario development and simulation. *Energy Procedia* 2015;76:565–72.
- [25] Kruck O, Crotogino F, Prelicz R, Rudolph T. Overview on all known underground storage technologies for hydrogen. In: *Project HyUnder—Assessment of the potential, the actors and relevant business cases for large scale and seasonal storage of renewable electricity by hydrogen underground storage in Europe*. Report D, vol. 3. 2013.
- [26] Tarkowski R, Czapowski G. Salt domes in Poland – Potential sites for hydrogen storage in caverns. *Int J Hydrog Energy* 2018;43(46):21414–27.
- [27] Acht A, Donadei S. Hydrogen storage in salt caverns state of the art, new developments and R&D projects. In: Bremen, Germany: SMRI fall 2012 technical conference. 2012.
- [28] Zivar D, Kumar S, Foroozesh J. Underground hydrogen storage: A comprehensive review. *Int J Hydrog Energy* 2021;46(45):23436–62.
- [29] Lord AS, Kobos PH, Borns DJ. Geologic storage of hydrogen: Scaling up to meet city transportation demands. *Int J Hydrog Energy* 2014;39(28):15570–82.
- [30] Fan L, Tu Z, Chan SH. Recent development of hydrogen and fuel cell technologies: A review. *Energy Rep* 2021;7:8421–46.
- [31] Heinemann N, Booth MG, Haszeldine RS, Wilkinson M, Scafidi J, Edlmann K. Hydrogen storage in porous geological formations – onshore play opportunities in the midland valley (Scotland, UK). *Int J Hydrog Energy* 2018;43(45):20861–74.
- [32] Hassanpouryouzband A, Joonaki E, Edlmann K, Haszeldine RS. Offshore geological storage of hydrogen: Is this our best option to achieve net-zero? *ACS Energy Lett* 2021;6(6):2181–6, Publisher: American Chemical Society.
- [33] Jafari Raad SM, Leonenko Y, Hassanzadeh H. Hydrogen storage in saline aquifers: Opportunities and challenges. *Renew Sustain Energy Rev* 2022;168:112846.
- [34] Navaid HB, Emadi H, Watson M. A comprehensive literature review on the challenges associated with underground hydrogen storage. *Int J Hydrog Energy* 2023;48(28):10603–35.

- [35] Tarkowski R, Uliasz-Misiak B. Towards underground hydrogen storage: A review of barriers. *Renew Sustain Energy Rev* 2022;162:112451.
- [36] Oldenburg CM, Pan L. Utilization of CO₂ as cushion gas for porous media compressed air energy storage. *Greenh Gases Sci Technol* 2013;3(2):124–35.
- [37] Heinemann N, Wilkinson M, Adie K, Edlmann K, Thaysen EM, Hassanpouryouzband A, et al. Cushion gas in hydrogen storage—A costly CAPEX or a valuable resource for energy crises? *Hydrogen* 2022;3(4):550–63.
- [38] Luboń K, Tarkowski R. Influence of capillary threshold pressure and injection well location on the dynamic CO₂ and H₂ storage capacity for the deep geological structure. *Int J Hydrog Energy* 2021;46(58):30048–60.
- [39] Ebigo A, Golfier F, Quintard M. A coupled, pore-scale model for methanogenic microbial activity in underground hydrogen storage. *Adv Water Resour* 2013;61:74–85.
- [40] Shi Z, Jessen K, Tsotsis TT. Impacts of the subsurface storage of natural gas and hydrogen mixtures. *Int J Hydrog Energy* 2020;45(15):8757–73.
- [41] Thiyagarajan SR, Emadi H, Hussain A, Patange P, Watson M. A comprehensive review of the mechanisms and efficiency of underground hydrogen storage. *J Energy Storage* 2022;51:104490.
- [42] Tarkowski R, Lankof L, Luboń K, Michalski J. Hydrogen storage capacity of salt caverns and deep aquifers versus demand for hydrogen storage: A case study of Poland. *Appl Energy* 2024;355:122268.
- [43] Sainz-García A, Abarca E, Rubi V, Grandia F. Assessment of feasible strategies for seasonal underground hydrogen storage in a saline aquifer. *Int J Hydrog Energy* 2017;42(26):16657–66.
- [44] Pfeiffer WT, al Hagrey SA, Köhn D, Rabbel W, Bauer S. Porous media hydrogen storage at a synthetic, heterogeneous field site: numerical simulation of storage operation and geophysical monitoring. *Environ Earth Sci* 2016;75(16):1177, .
- [45] Hagemann B, Rasoulzadeh M, Panfilov M, Ganzer L, Reitenbach V. Mathematical modeling of unstable transport in underground hydrogen storage. *Environ Earth Sci* 2015;73(11):6891–8, .
- [46] Luboń K, Tarkowski R. Numerical simulation of hydrogen injection and withdrawal to and from a deep aquifer in NW Poland. *Int J Hydrog Energy* 2020;45(3):2068–83.
- [47] Mahdi DS, Al-Khdheawi EA, Yuan Y, Zhang Y, Iglauer S. Hydrogen underground storage efficiency in a heterogeneous sandstone reservoir. *Adv Geo- Energy Res* 2021;5(4):437–43, .
- [48] Heinemann N, Scafidi J, Pickup G, Thaysen E, Hassanpouryouzband A, Wilkinson M, et al. Hydrogen storage in saline aquifers: The role of cushion gas for injection and production. *Int J Hydrog Energy* 2021;46(79):39284–96.
- [49] Hagemann B, Rasoulzadeh M, Panfilov M, Ganzer L, Reitenbach V. Hydrogenization of underground storage of natural gas. *Comput Geosci* 2016;20(3):595–606.
- [50] Scafidi J, Wilkinson M, Gilfillan SMV, Heinemann N, Haszeldine RS. A quantitative assessment of the hydrogen storage capacity of the UK continental shelf. *Int J Hydrog Energy* 2021;46(12):8629–39.
- [51] CMGL-GEM. GEM software. 2023, <https://www.cmgl.ca/gem>.
- [52] Thaysen EM, Armitage T, Slabon L, Hassanpouryouzband A, Edlmann K. Microbial risk assessment for underground hydrogen storage in porous rocks. *Fuel* 2023;352:128852.
- [53] Panfilov M. Underground storage of hydrogen: In situ self-organisation and methane generation. *Transp Porous Media* 2010;85(3):841–65, .
- [54] Tremosa J, Jakobsen R, Le Gallo Y. Assessing and modeling hydrogen reactivity in underground hydrogen storage: A review and models simulating the Lobodice town gas storage. *Front Energy Res* 2023;11.
- [55] Peng D-Y, Robinson DB. A new two-constant equation of state. *Ind Eng Chem Fundam* 1976;15(1):59–64.
- [56] Thaysen EM, Butler IB, Hassanpouryouzband A, Freitas D, Alvarez-Borges F, Krevor S, et al. Pore-scale imaging of hydrogen displacement and trapping in porous media. *Int J Hydrog Energy* 2023;48(8):3091–106.
- [57] Pan B, Liu K, Ren B, Zhang M, Ju Y, Gu J, et al. Impacts of relative permeability hysteresis, wettability, and injection/withdrawal schemes on underground hydrogen storage in saline aquifers. *Fuel* 2023;333:126516.
- [58] Safari A, Zeng L, Nguele R, Sugai Y, Sarmadivaleh M. Review on using the depleted gas reservoirs for the underground H₂ storage: A case study in Niigata prefecture, Japan. *Int J Hydrog Energy* 2023;48(28):10579–602.
- [59] Juanes R, Spiteri EJ, Orr Jr FM, Blunt MJ. Impact of relative permeability hysteresis on geological CO₂ storage. *Water Resour Res* 2006;42(12).
- [60] Chabab S, Théveneau P, Coquelet C, Corvisier J, Paricaud P. Measurements and predictive models of high-pressure H₂ solubility in brine (H₂O+NaCl) for underground hydrogen storage application. *Int J Hydrog Energy* 2020;45(56):32206–20.
- [61] Lucia MD, Pilz P, Liebscher A, Kühn M. Measurements of H₂ solubility in saline solutions under reservoir conditions: Preliminary results from project H2STORE. *Energy Procedia* 2015;76:487–94.
- [62] Wang G, Pickup G, Sorbie K, Mackay E. Numerical modelling of H₂ storage with cushion gas of CO₂ in subsurface porous media: Filter effects of CO₂ solubility. *Int J Hydrog Energy* 2022;47(67):28956–68.
- [63] Sander R. Compilation of Henry's law constants, version 3.99. *Gases/Laboratory Studies/Troposphere/Chemistry (chemical composition and reactions)*; 2014.
- [64] de Moegen H, Giouse H. Long-term study of cushion gas replacement by inert gas. In: *Proceedings of the 64th annual technical conference and exhibition of the society of petroleum engineers*. 1989, p. 12.
- [65] Tek MR. *Underground storage of natural gas: theory and practice*, no. 171. Springer Science & Business Media; 1989.
- [66] Feldmann F, Hagemann B, Ganzer L, Panfilov M. Numerical simulation of hydrodynamic and gas mixing processes in underground hydrogen storages. *Environ Earth Sci* 2016;75(16):1165, .
- [67] Hemme C, Van Berk W. Hydrogeochemical modeling to identify potential risks of underground hydrogen storage in depleted gas fields. *Appl Sci* 2018;8(11):2282, Number: 11 Publisher: Multidisciplinary Digital Publishing Institute.
- [68] Gelhar LW, Welty C, Rehfeldt KR. A critical review of data on field-scale dispersion in aquifers. *Water Resour Res* 1992;28(7):1955–74, _eprint: <https://onlinelibrary.wiley.com/doi/pdf/10.1029/92WR00607>.
- [69] Sigmund PM. Prediction of molecular diffusion at reservoir conditions. II. estimating the effects of molecular diffusion and convective mixing in multicomponent systems. *J Can Pet Technol(Canada)* 1976;15(3).
- [70] Lekkala SR. *Impact of injecting inert cushion gas into a gas storage reservoir*. West Virginia University; 2009.
- [71] Paterson L. The implications of fingering in underground hydrogen storage. *Int J Hydrog Energy* 1983;8(1):53–9.
- [72] Okoroafor ER, Saltzer SD, Kovscek AR. Toward underground hydrogen storage in porous media: Reservoir engineering insights. *Int J Hydrog Energy* 2022;47(79):33781–802.
- [73] Yousefi SH, Groenenberg R, Koornneef J, Juez-Larré J, Shahi M. Techno-economic analysis of developing an underground hydrogen storage facility in depleted gas field: A Dutch case study. *Int J Hydrog Energy* 2023;S0360319923018256.